

Supplementary information

Rational design of near-infrared fluorophores with phenolic D–A type structure and construction of a fluorescent probe for cysteine imaging

Dugang Chen,^{a,#,*} Gang Nie,^{b,#} Yecheng Dang,^a Wenjie Liang,^a Wanqing Li,^a Cheng Zhong^{c,*}

^a Key Laboratory for Green Chemical Process of Ministry of Education, School of Chemical Engineering and Pharmacy, Wuhan Institute of Technology, Wuhan 430205, P. R. China

^b Hubei Key Laboratory of Nature Medicinal Chemistry and Resource Evaluation, Tongji Medical College of Pharmacy, Huazhong University of Science and Technology, Wuhan 430030, P. R. China

^c College of Chemistry and Molecular Science, Wuhan University, Wuhan 430072, P. R. China.

These authors contributed equally.

*Correspondence to:

D. Chen (E-mail: dg.chen@wit.edu.cn) or C. Zhong (zhongcheng@whu.edu.cn)

Contents:

Materials and instruments

Preparation of solutions

Fluorescence quantum yield

pKa measurements

Theoretical calculations

Cytotoxicity assays

Cell culture and cell imaging

In vivo imaging

Synthesis

Fig. S1 ¹H NMR and ¹³C NMR spectra of the four fluorophores.

Fig. S2 ¹H NMR and ¹³C NMR of ANTC.

Fig. S3 Mass spectrum of ANTC.

Fig. S4 UV–vis and fluorescence spectra of HNTC-1,2 and HNTC-1,4 in DMSO with 10% of Et₃N or 10% of HAc.

Fig. S5 Charge distributions of each atom in HNTC-2,6, HNTC-1,2 and HNTC-1,4.

Fig. S6 Time-dependent fluorescence spectra of ANTC with the addition of Cys, Hcy and GSH; fluorescence responses of ANTC in the presence of different interferences; and fluorescence changes of ANTC with the gradual addition of Cys.

Fig. S7 pH-dependent fluorescence spectra of ANTC in the absence and presence of Cys; and the photostability of HNTC-1,4 under light irradiation.

Fig. S8 Viability of HeLa cells when incubated with ANTC in different concentrations for 24 h.

Fig. S9 Living cell imaging in HepG2 cells.

Table S1 Property comparisons of recently reported probes with the acrylate group as the recognition site in the presence of Cys.

Materials and instruments

All the solvents and reagents were obtained commercially. Fluorescence spectra were recorded on a Hitachi F-4500 spectrometer. UV–vis absorption spectra were recorded on a PerkinElmer Lambda 365 spectrophotometer. The pH measurements were made with a LEITING PHSJ-3F pH meter. Fluorescence imaging was carried out by a confocal laser scanning microscope (ZEISS LSM880). *In vivo* imaging assays were performed in a small-animal *in vivo* imaging system (Pearl Imager, LICOR, USA). ¹H NMR spectra were recorded on Bruker Ascend 400 MHz spectrometers, and ¹³C NMR spectra were recorded on 100 MHz spectrometers. Mass spectra were recorded on a GCMS-QP2020 instrument.

Preparation of solutions

The fluorophores were dissolved in different solvents respectively with concentration of 1 mM as the stock solution. The probe was dissolved in DMSO to afford 1 mM stock solution. Other analytes, including Cys, Hcy, NaCl, KCl, H₂O₂, NaClO, N₂H₄, vitamin C, glycine, glutamic acid, histidine, proline, lysine, glucose, Na₂S, and Na₂SO₃, were dissolved in deionized water to afford 10 mM aqueous solution. GSH were dissolved in deionized water to afford 10 mM or 100 mM aqueous solution, respectively.

Fluorescence quantum yield

The fluorescence quantum yield (Φ) indicates the ability of a substance to emit fluorescence and is a very important parameter of the probe. The calculation formula is:

$$\phi_{unk} = \phi_{std} \left(\frac{I_{unk}}{A_{unk}} \right) \left(\frac{A_{std}}{I_{std}} \right) \left(\frac{\eta_{unk}}{\eta_{std}} \right)^2$$

where, Φ_{unk} is the fluorescence quantum yield of the probe, Φ_{std} is the reference quantum yield (rhodamine b in methanol), I_{unk} and I_{std} the integral fluorescence intensity of the probe and reference, A_{unk} and A_{std} the absorbance of the probe and reference, η_{unk} and η_{std} the refractive index of the corresponding solution of the probe and the reference, respectively.

pKa measurements

The pKa of four dyes were measured by UV-vis spectrophotometry. It was calculated through the following formula:

$$\text{pKa} = \text{pH} + \lg(A - A_B) / (A_{HB} - A),$$

The dye (HB) ionizes in solution: $\text{HB} = \text{H}^+ + \text{B}^-$

The following absorbance values were obtained at a certain wavelength. A_B refers to the absorbance of the dye in high pH solution, where only the form of B^- exists. A_{HB} refers to the absorbance of the dye in low pH solution, where only the form of HB exists. A refers to the absorbance of the dye in an appropriate pH solution, where HB and B^- coexist. The UV-vis spectra of each dye in different pH buffers were tested, and a mean value of pKa was calculated.

Theoretical calculations

All optimizations of ground states were done at PBE0/def2-SVP level with Grimme's D3BJ empirical dispersion correction. Then the vertical excited states were calculated at same level with TDDFT. All the calculations were performed using Gaussian 09 program and the hole-electron

distribution analysis was performed using the Multiwfn program.

Cytotoxicity assays

The cell viability of the probe on HeLa cells was examined by MTT assay. Briefly, cells were seeded in 96-well microplates at a density of 5×10^3 cells/well in 100 μL of complete MEM media and incubated at 37 °C in an atmosphere containing 5% CO_2 and 95% air. After the cells reached about 80% confluency, the cells were incubated with 0, 2, 5, 10, 20 and 30 μM of the probe for 24 h. After that, 20 μL of MTT solution (5 mg mL^{-1}) in PBS was added to each well and further cultured for another 4 h at 37 °C. Then the MEM solution was removed and 150 μL of DMSO was added to dissolve the formed purple crystals derived from MTT. The plates were then analyzed with a microplate reader (Tecan, Spark 10M) at the absorbance wavelength of 570 nm.

Cell culture and cell imaging

HeLa cells were obtained from iCell Bioscience Inc. HeLa cells were maintained under the standard culture conditions (atmosphere of 5% CO_2 and 95% air at 37°C) in MEM medium (Corning), supplemented with 10% FBS (Biological Industries).

Before confocal microscopy imaging of cells with probes, HeLa cells in the exponential phase were plated on 35 mm glass-bottom culture dishes for 2 days to reach around 80% confluency, respectively. Cell culture was maintained at 37 °C under an atmosphere of 5% CO_2 and 95% air for desired time. Culture medium was changed every two days to keep the exponential growth of the cells. On the day of treatment, the cells were incubated with the appropriate concentrations of probe or additives for different time at 37 °C and washed with 1 mL of PBS for three times at room temperature, then they were added to 1 mL of PBS culture medium and observed under confocal microscopy with a 63 \times oil-immersion objective.

***In vivo* imaging**

Male C57BL/6J (20 g-25 g) mice were purchased from the Center for Experimental Animal Research (Wuhan, China). The animal experiments were approved by the Institutional Animal Care and Use Committee of Tongji Medical College, Huazhong University of Science and Technology (permit number: SCXK (Hubei) 2017–0012). The animal care and experimental procedures were carried out in accordance with the Guidelines of the Institutional Animal Care and Use Committee of Tongji Medical College and the National Institutes of Health Guide for the Care and Use of Laboratory Animals. All male C57BL/6J (20–25 g) mice were adaptive feeding for one week after arrival.

C57BL/6J mice were divided into three groups. All the reagents were injected intraperitoneally. The control group mice were injected with saline for 15 min; ANTC group mice were injected with ANTC (200 μM , 200 μL in 1:99 DMSO/saline, v/v) and incubated for 30 min; Cys+ANTC group mice were pre-injected with Cys (1 mM, 200 μL) for 15 min and then with ANTC (200 μM , 200 μL in 1:99 DMSO/saline, v/v) for 30 min. The fluorescent images of the C57BL/6J mice were obtained by a small-animal *in vivo* imaging system.

Synthesis

2-(3,5,5-trimethylcyclohex-2-en-1-ylidene)malononitrile (Dicyanoisophorone)[1]: Isophorone (10 g, 72.35 mmol) and malononitrile (5.74 g, 86.82 mmol) were dissolved in absolute ethanol (40 mL)

under an argon atmosphere, followed by the addition of piperidine (1.2 mL) and acetic acid (1.7 mL). Then the mixture was heated to 80 °C and stirred for 12 h. After being cooled to room temperature, the mixture was neutralized with acetic acid, precipitates were removed by filtration. The mixture was concentrated under reduced pressure to remove half of the ethanol in the mixture and then placed at 4 °C for 1 h. Thus, the precipitated crystals were filtered. The pure compound **1** was obtained by recrystallization. Yield: 11.7 g, 87%. ¹H NMR (400 MHz, CDCl₃) δ [ppm]: 6.62 (dd, *J* = 4 Hz, 1H), 2.51(s, 2H), 2.24(s, 2H), 2.03(d, 3H), 1.01(s, 6H).

2-(3-(2-(6-hydroxynaphthalen-2-yl)vinyl)-5,5-dimethylcyclohex-2-en-1-ylidene)malononitrile 2,5-dibromothiopheno[3,2-*b*]thiophene (**HNTC-2,6**)[2]: Dicyanoisophorone (1 g, 5.37 mmol) and 6-hydroxy-2-naphthaldehyde (1.11 g, 6.44 mmol) were dissolved in absolute ethanol (15 mL) under an argon atmosphere, followed by the addition of piperidine (0.5 mL) and acetic acid (0.7 mL). Then the mixture was heated to 80 °C and stirred for 12 h. After cooled to room temperature, the mixture was neutralized with acetic acid, diluted by dichloromethane and washed with water twice. The organic layer was collected and dried with anhydrous Na₂SO₄. After the solvent was evaporated, the residue was purified by silica column chromatography using petroleum ether/ethyl acetate (v/v, 4/1) as eluent. Yield: 0.96 g, 52%. ¹H NMR (400 MHz, DMSO-*d*₆) δ [ppm]: 10.00 (s, 1H), 8.02 (s, 1H), 7.82-7.76 (m, 2H), 7.70 (d, *J* = 8 Hz, 1H), 7.49-7.38 (m, 2H), 7.13-7.10 (m, 2H), 6.90 (s, 1H), 2.60 (d, *J* = 16 Hz, 4H), 1.03 (s, 6H). ¹³C NMR (100 MHz, DMSO-*d*₆) δ [ppm]: 170.72, 157.15, 156.67, 138.69, 135.79, 131.04, 130.67, 129.65, 128.82, 128.05, 127.24, 124.72, 122.69, 119.73, 114.48, 113.67, 109.54, 76.07, 42.76, 38.65, 32.14, 27.92. MS for C₂₃H₂₀N₂O [M]⁺, calculated: 340.16; found: 340.20.

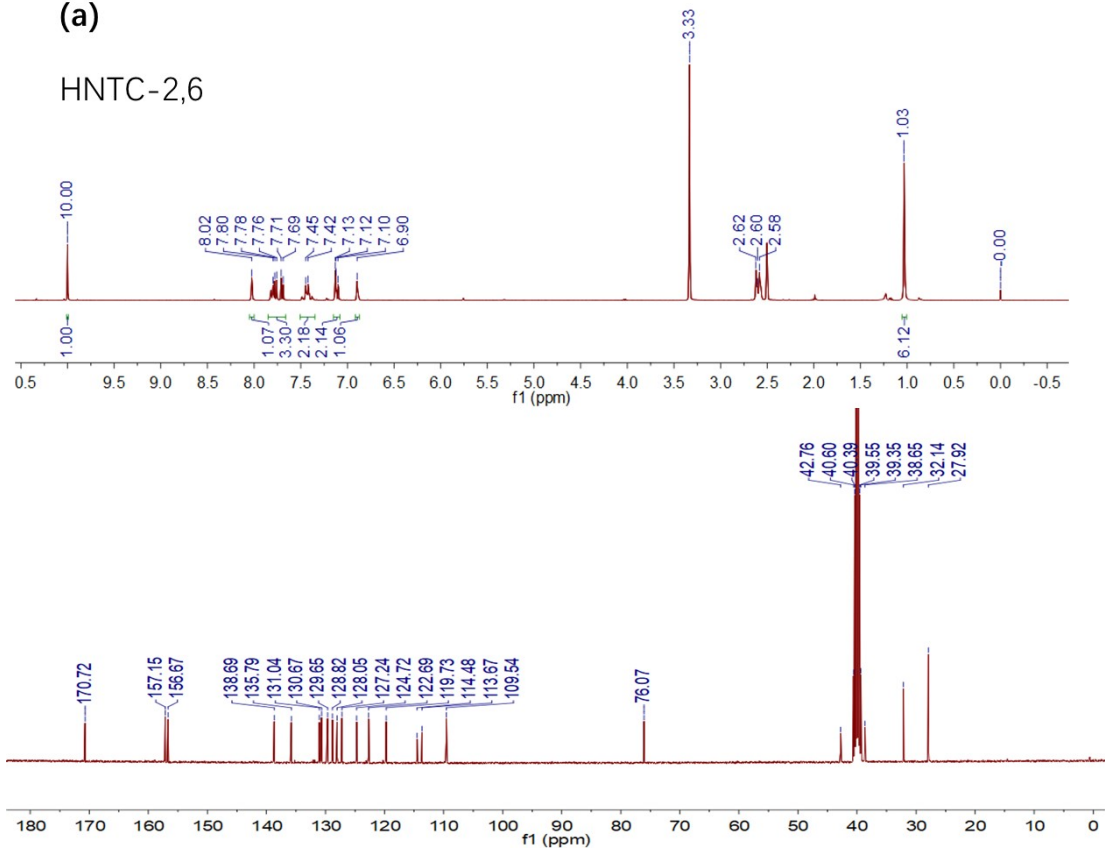
2-(3-(2-(2-hydroxynaphthalen-1-yl)vinyl)-5,5-dimethylcyclohex-2-en-1-ylidene)malononitrile (**HNTC-1,2**)[3]: **HNTC-1,2** was prepared with the same method as **HNTC-2,6**, except that the starting materials were **TC** (1 g, 5.37 mmol) and 2-hydroxy-1-naphthaldehyde (1.11 g, 6.44 mmol). Yield: 1.27 g, 69%. ¹H NMR (400 MHz, DMSO-*d*₆) δ [ppm]: 10.65 (s, 1H), 8.02 (d, *J* = 8 Hz, 1H), 7.84-7.79 (m, 3H), 7.57-7.52 (m, 2H), 7.36 (t, *J* = 14 Hz, 1H), 7.26 (d, *J* = 8 Hz, 1H), 6.75 (s, 1H), 2.71 (s, 2H), 2.62 (s, 2H), 1.07 (s, 6H). ¹³C NMR (100 MHz, DMSO-*d*₆) δ [ppm]: 170.79, 157.61, 156.10, 133.89, 133.00, 131.95, 131.73, 129.15, 128.63, 127.71, 123.66, 123.29, 122.37, 118.87, 114.78, 75.86, 42.89, 38.31, 32.15, 27.95. MS for C₂₃H₂₀N₂O [M]⁺, calculated: 340.16; found: 340.20.

2-(3-(2-(4-hydroxynaphthalen-1-yl)vinyl)-5,5-dimethylcyclohex-2-en-ylidene)malononitrile (**HNTC-1,4**)[4]: **HNTC-1,4** was prepared with the same method as **HNTC-2,6**, except that the starting materials were dicyanoisophorone (1 g, 5.37 mmol) and 4-hydroxy-1-naphthaldehyde (1.11 g, 6.44 mmol). The residue was purified by silica column chromatography using petroleum ether/ethyl acetate (v/v, 3/1) as eluent. Yield: 0.53 g, 29%. ¹H NMR (400 MHz, DMSO-*d*₆) δ [ppm]: 10.77 (s, 1H), 8.36 (d, *J* = 8 Hz, 1H), 8.18 (d, *J* = 8 Hz, 1H), 8.01-7.96 (m, 2H), 7.59 (t, *J* = 14 Hz, 1H), 7.50 (t, *J* = 14 Hz, 1H), 7.33 (d, *J* = 16 Hz, 1H), 6.93 (d, *J* = 8 Hz, 1H), 6.85 (s, 1H), 2.71 (s, 2H), 2.60 (s, 2H), 1.04 (s, 6H). ¹³C NMR (100 MHz, DMSO-*d*₆) δ [ppm]: 170.79, 157.44, 156.19, 134.49, 128.86, 127.70, 126.76, 125.46, 123.73, 122.24, 114.67, 113.83, 109.14, 100.10, 75.30, 42.89, 38.64, 32.20, 27.96. MS for C₂₃H₂₀N₂O [M]⁺, calculated: 340.16; found: 340.15.

2-(3-(4-hydroxystyryl)-5,5-dimethylcyclohex-2-en-1-ylidene)malononitrile (HBTC-1,4)[5]:
HBTC-1,4 was prepared with the same method as HNTC-2,6, except that the starting materials were dicyanoisophorone (1 g, 5.37 mmol) and 4-hydroxybenzaldehyde (0.79 g, 6.44 mmol). The residue was purified by silica column chromatography using dichloromethane as eluent. Yield: 0.81 g, 64%. ¹H NMR (400 MHz, DMSO-*d*₆) δ [ppm]: 9.98 (s, 1H), 7.56 (d, *J* = 8 Hz, 2H), 7.21 (d, *J* = 4 Hz, 2H), 6.81-6.87 (m, 3H), 2.60 (s, 2H), 2.53 (s, 2H), 1.01 (s, 6H). ¹³C NMR (100 MHz, DMSO-*d*₆) δ [ppm]: 170.75, 159.81, 157.19, 138.76, 130.35, 127.59, 126.72, 121.85, 116.35, 114.61, 113.79, 75.27, 42.79, 38.66, 32.13, 27.91. MS for C₁₉H₁₈N₂O [M]⁺, calculated: 290.14; found: 290.15.

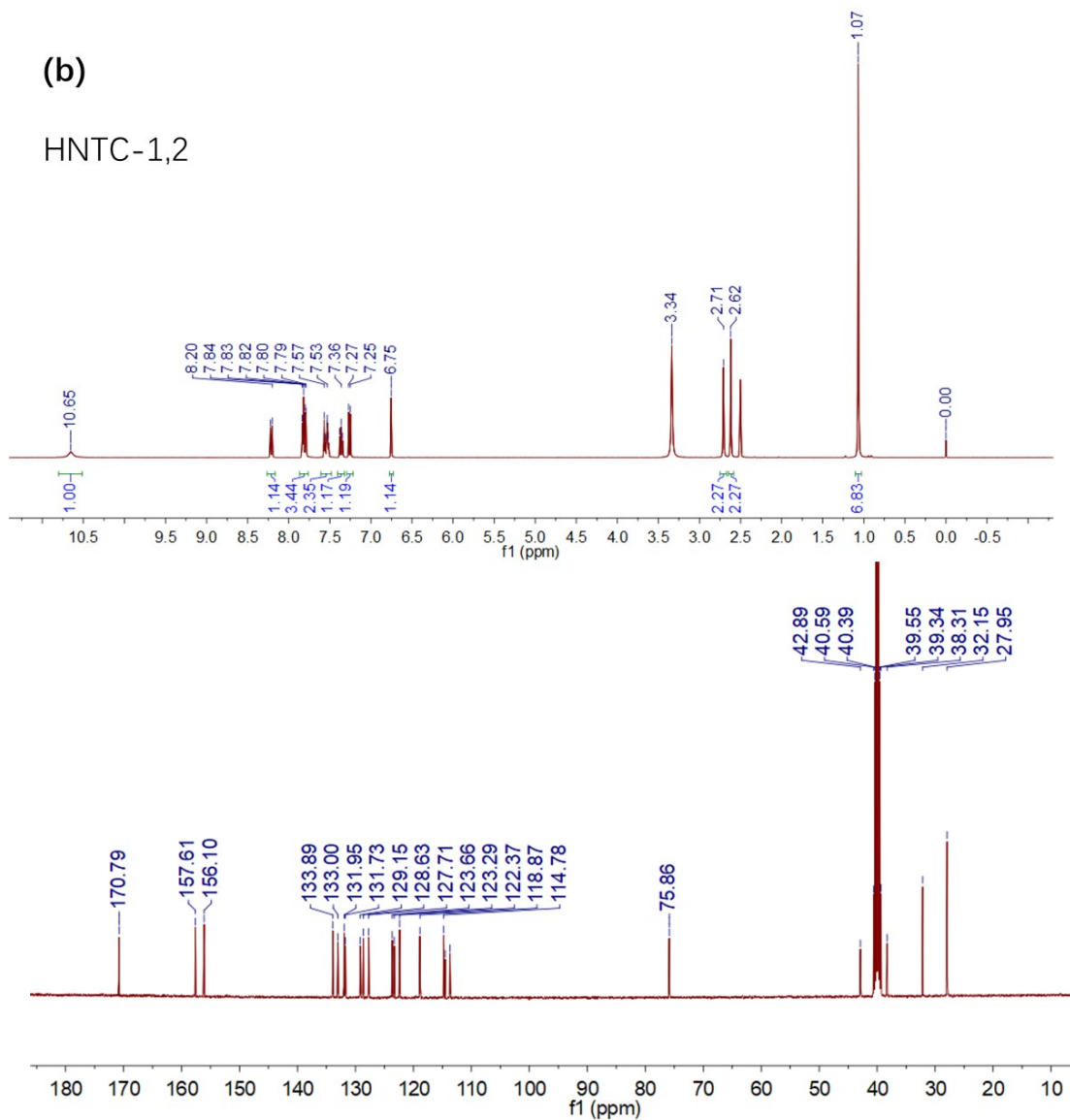
(a)

HNTC-2,6



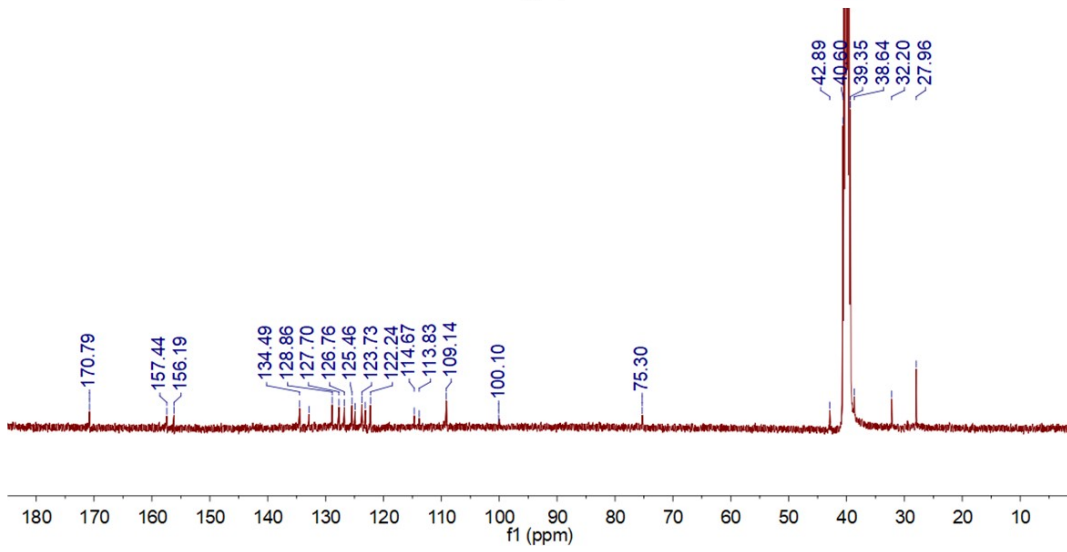
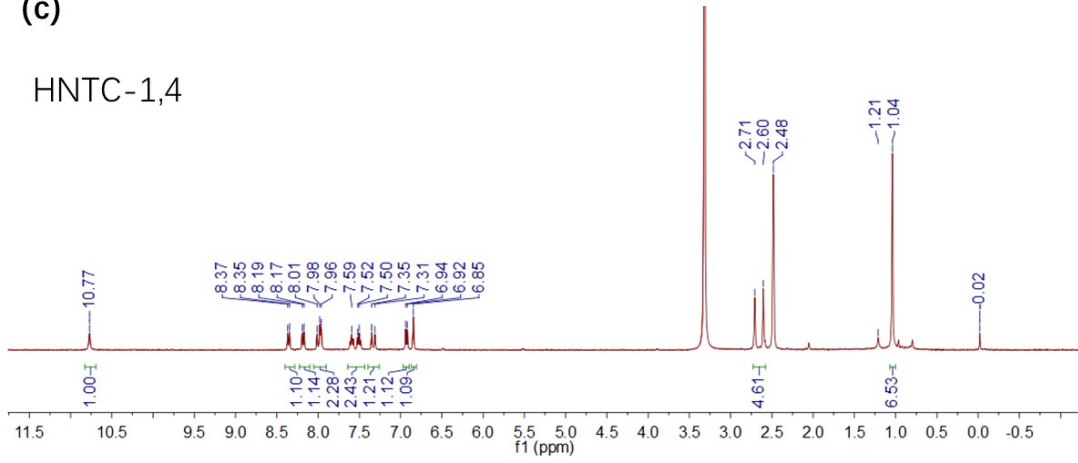
(b)

HNTC-1,2



(c)

HNTC-1,4



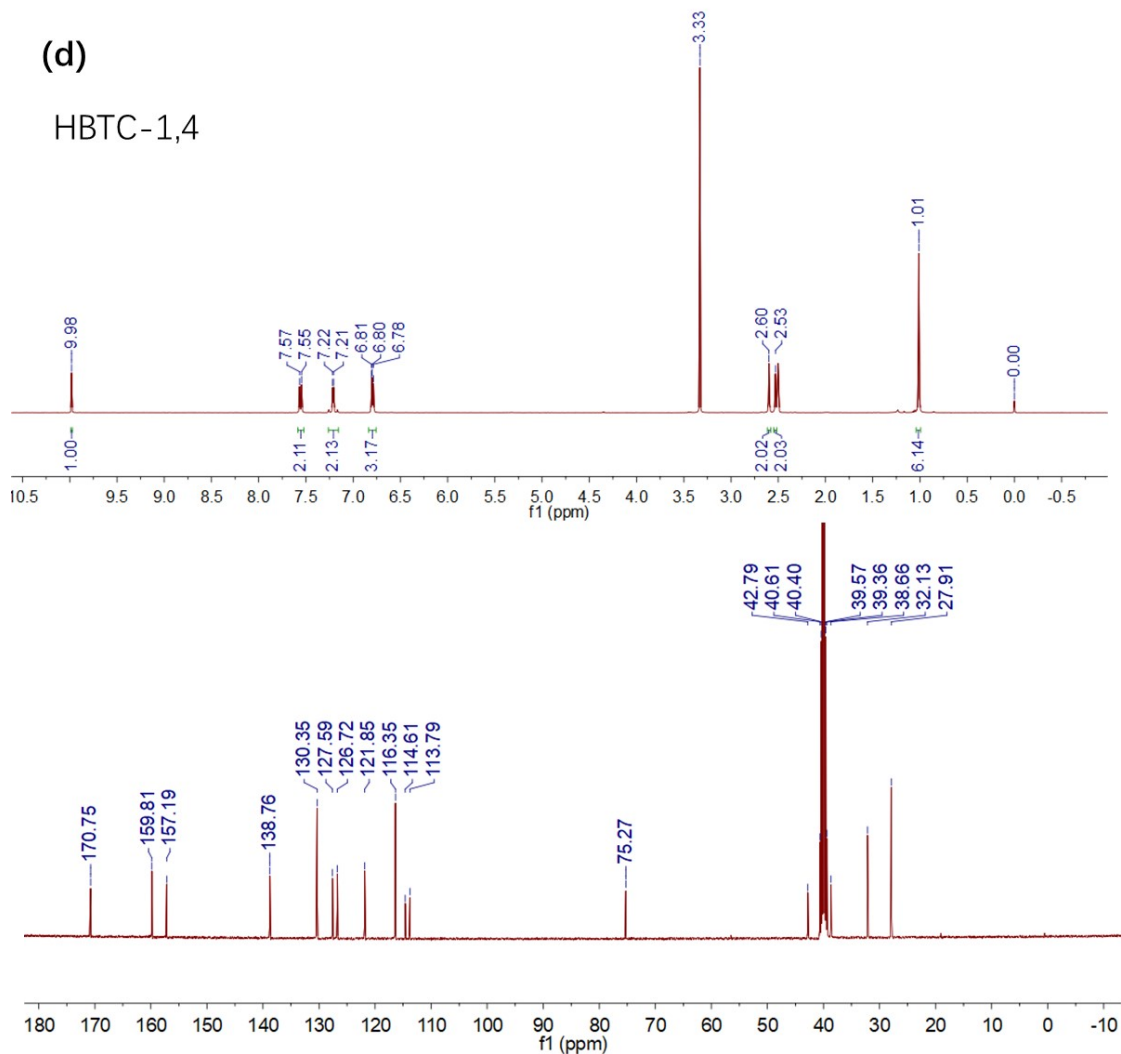


Fig. S1 ^1H NMR and ^{13}C NMR of (a) HNTC-2,6, (b) HNTC-1,2, (c) HNTC-1,4 and (d) HBTC-1,4 in $\text{DMSO-}d_6$.

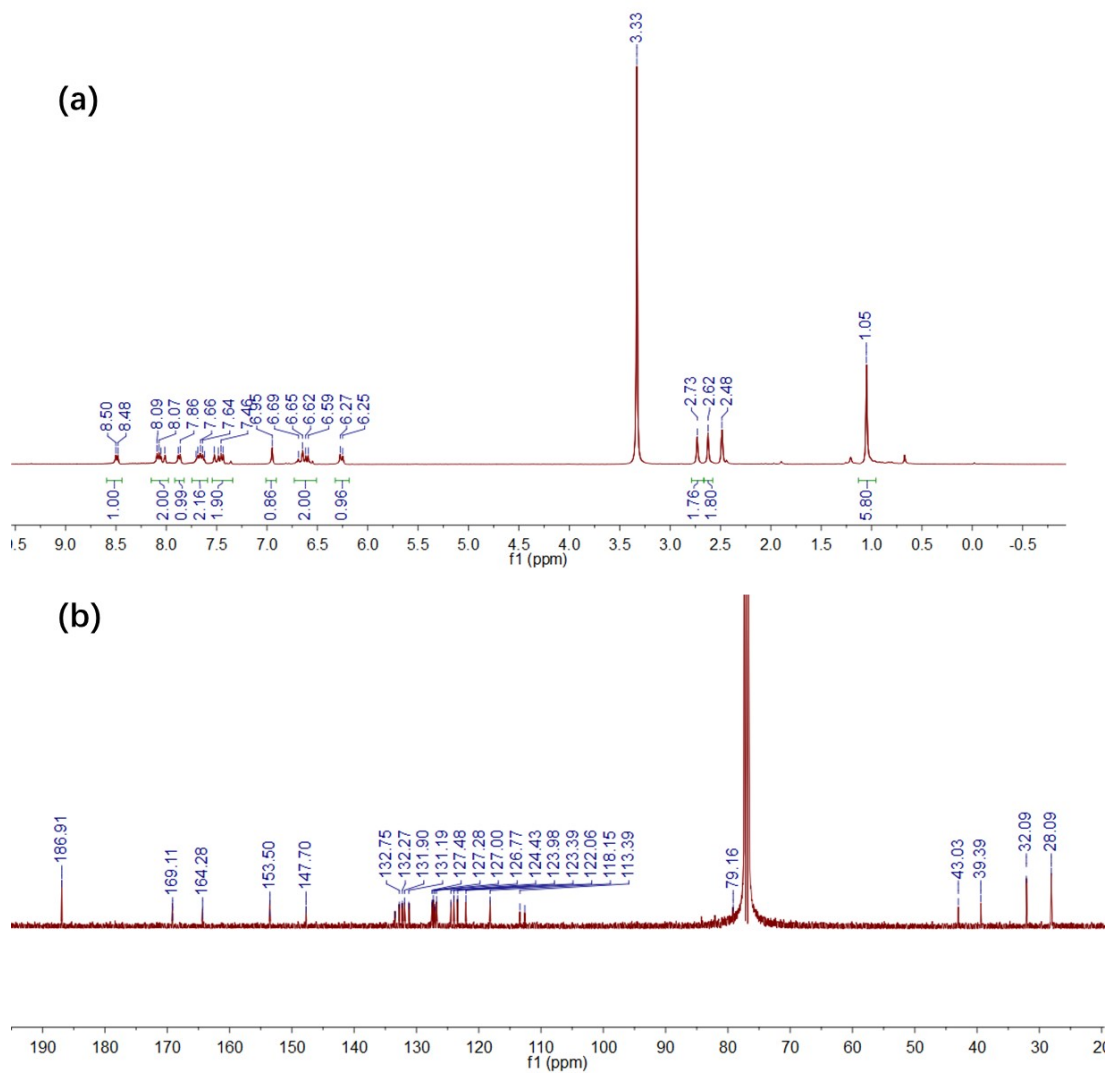


Fig. S2 (a) ^1H NMR in $\text{DMSO-}d_6$ and (b) ^{13}C NMR in CDCl_3 of ANTC.

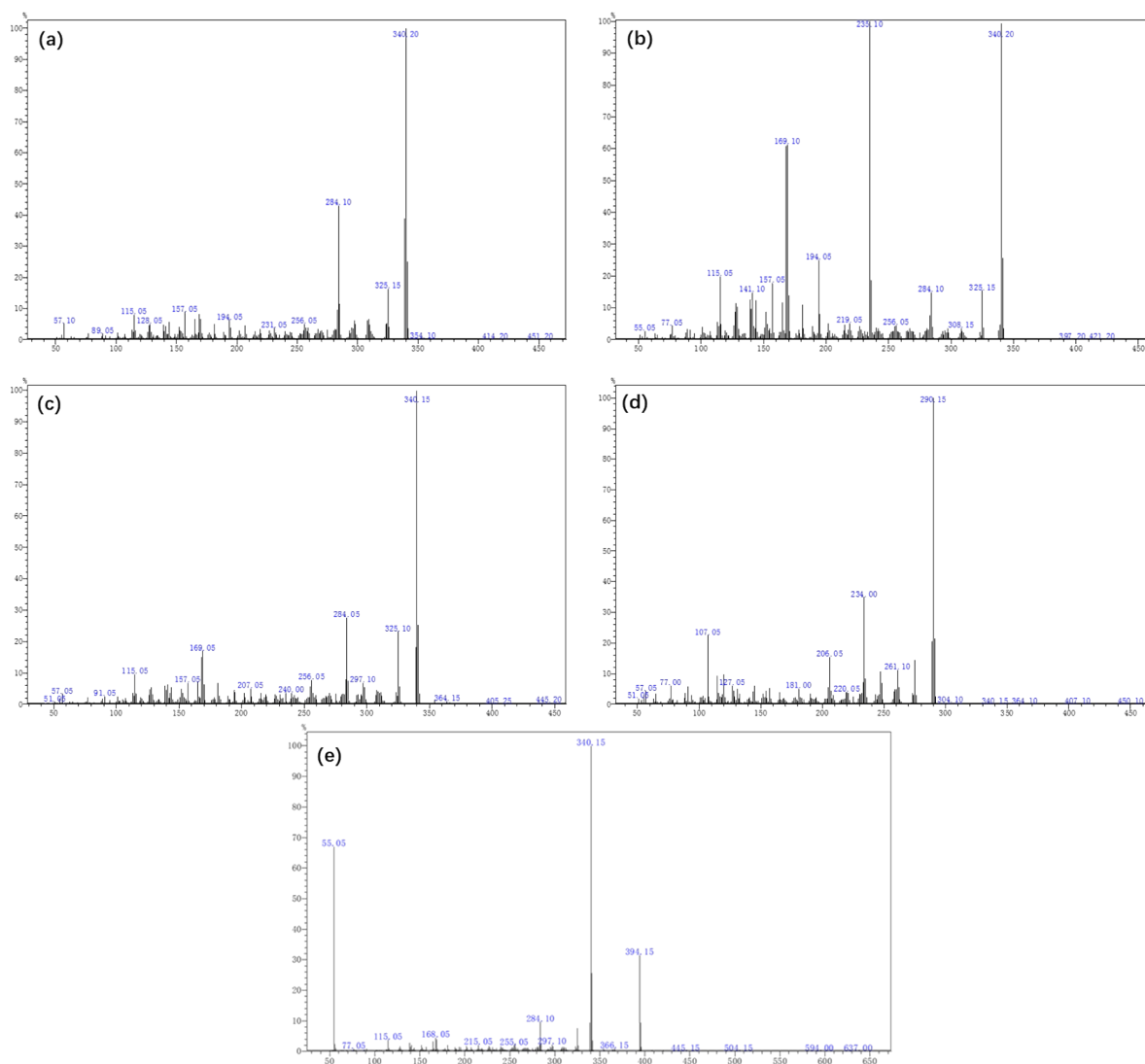


Fig. S3 Mass spectrum of (a) HNTC-2,6, (b) HNTC-1,2, (c) HNTC-1,4 (d) HBTC-1,4 and (e) ANTC.

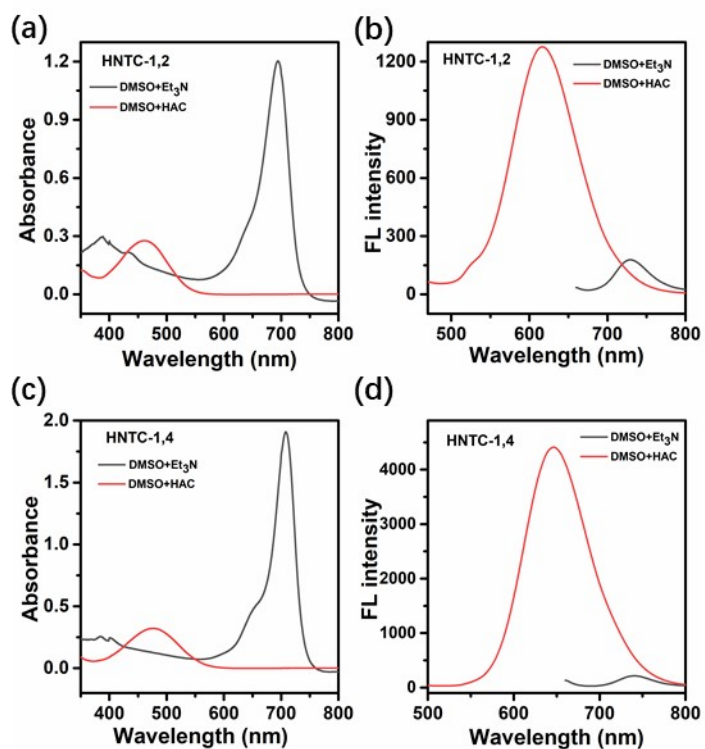


Fig. S4 UV-vis and fluorescence spectra of (a) (b) HNTC-1,2 and (c) (d) HNTC-1,4 in DMSO with 10% of Et₃N or 10% of HAc. Concentration: 10 μM.

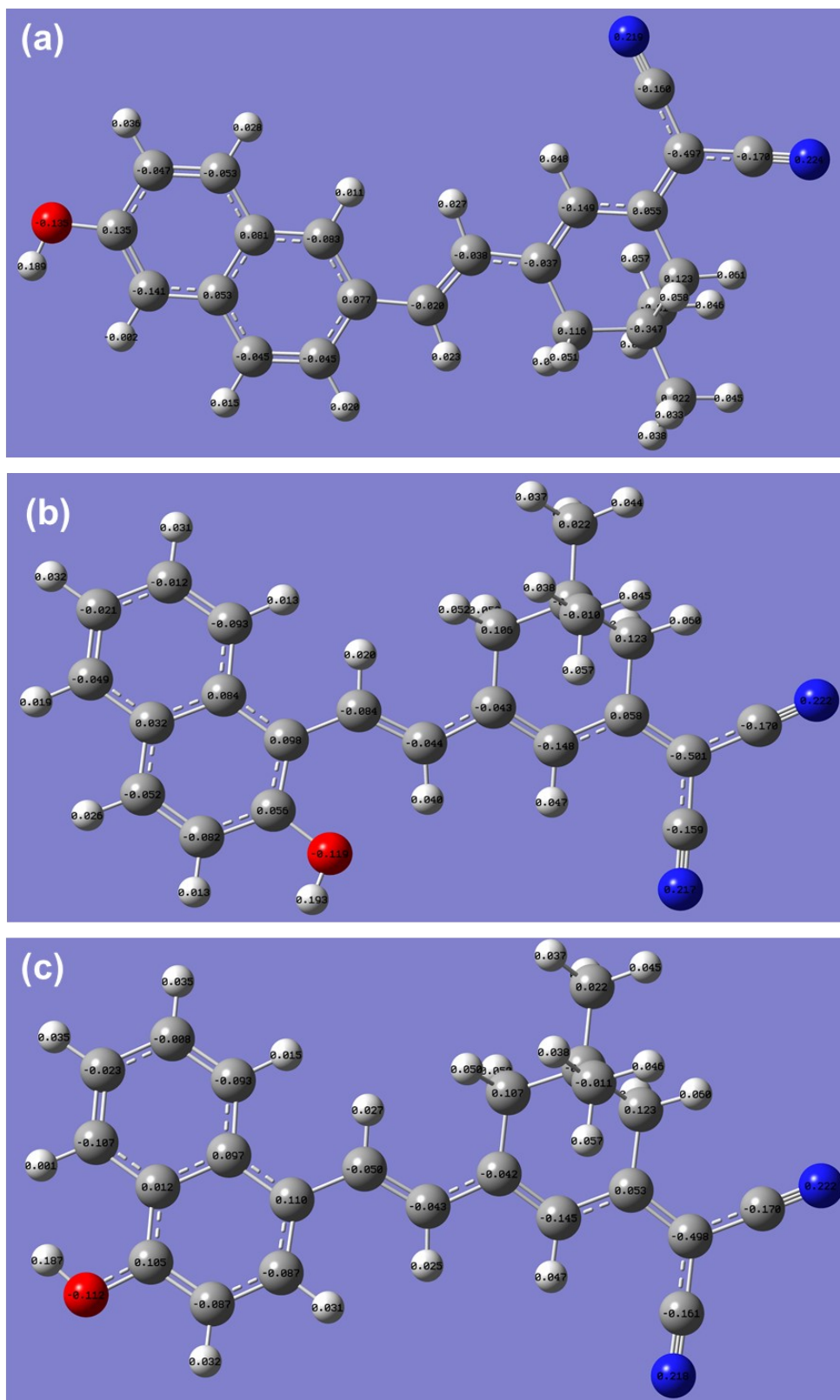


Fig. S5 Charge distributions of each atoms in (a) HNTC-2,6, (b) HNTC-1,2, and (c) HNTC-1,4 in

the ground state.

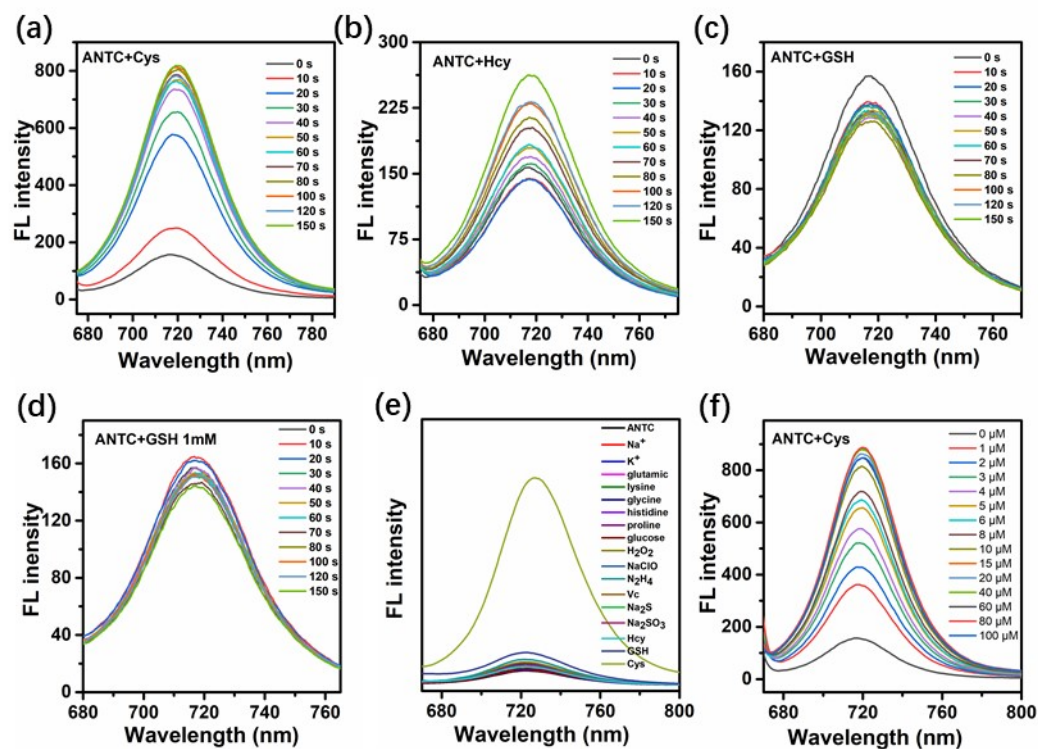


Fig. S6 Time-dependent fluorescence spectra of ANTC (10 μM) with the addition of (a) Cys (10 μM), (b) Hcy (100 μM), (c) GSH (100 μM) and (d) GSH (1 mM); (e) fluorescence responses of ANTC (10 μM) in the presence of different analytes (100 μM); (f) fluorescence changes of ANTC with the gradual addition of Cys (1-100 μM).

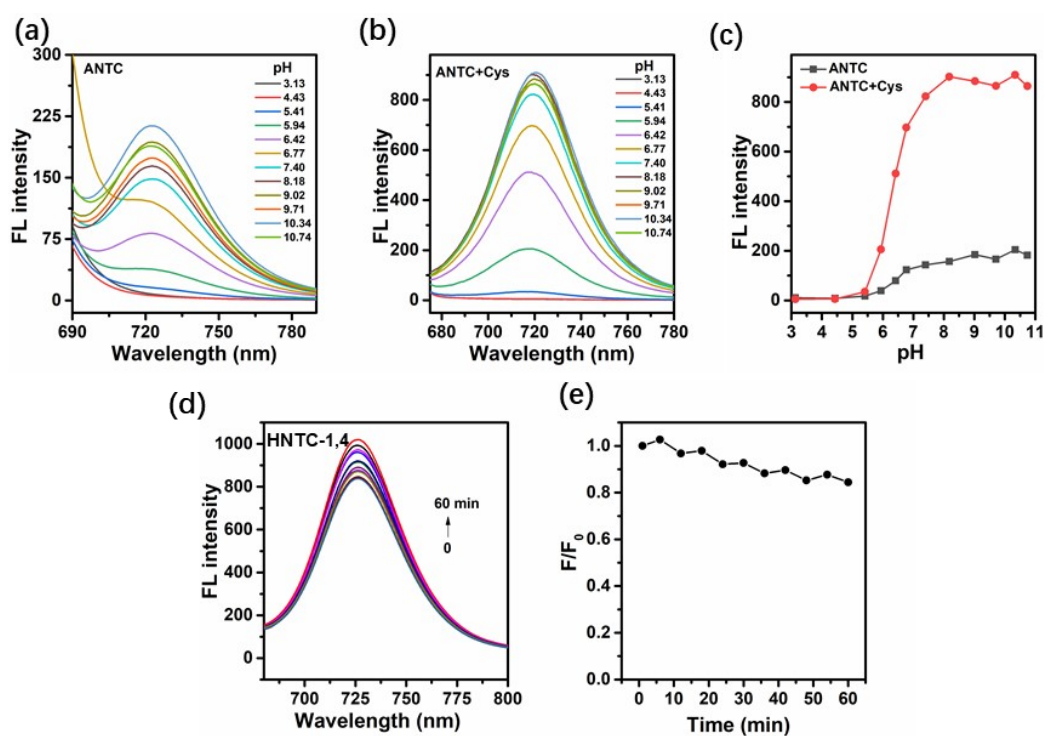


Fig. S7 pH-dependent fluorescence spectra of (a) ANTC and (b) ANTC with the addition of Cys; (c) pH-dependent fluorescence intensity changes of ANTC and ANTC with Cys; changes of (d) the fluorescence spectra and (e) fluorescence intensity of HNTC-1,4 under light irradiation in 60 min (Xe lamp, 150 w, 650 nm).

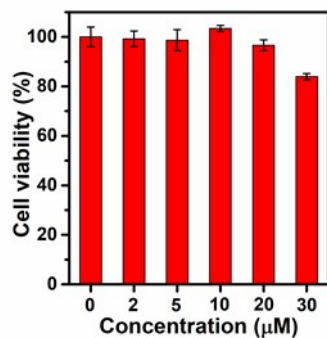


Fig. S8 Viability of HeLa cells when incubated with ANTC in different concentrations for 24 h.

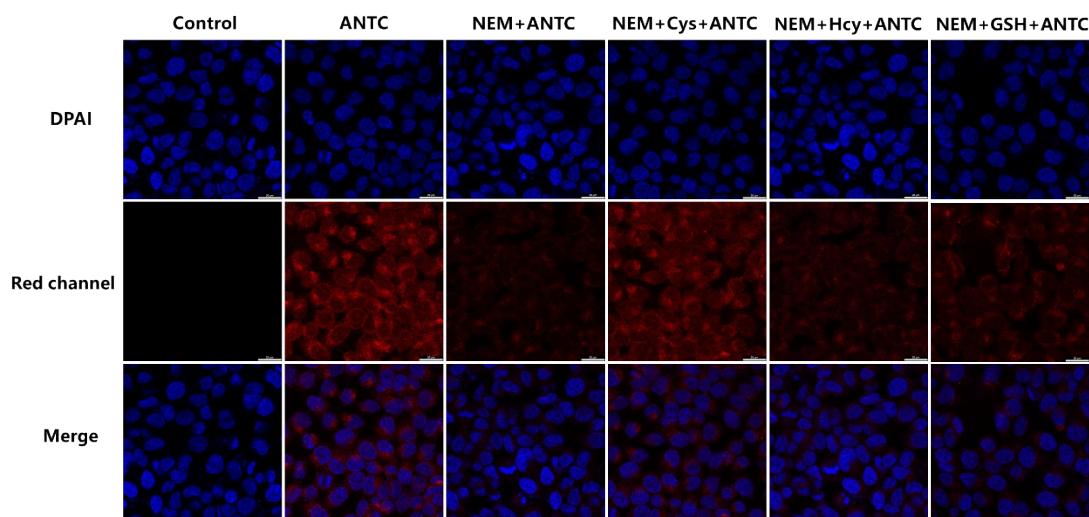
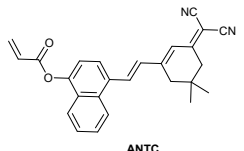
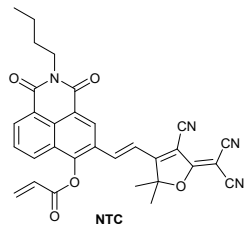
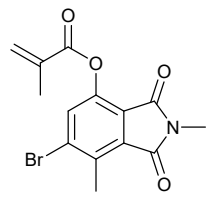
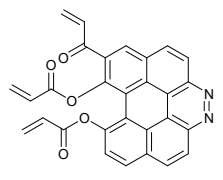
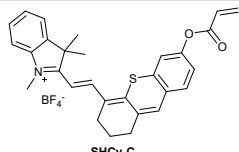
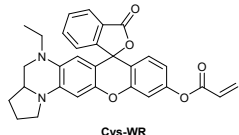
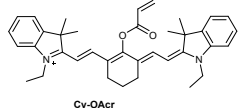
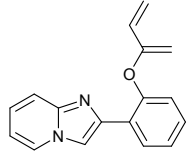
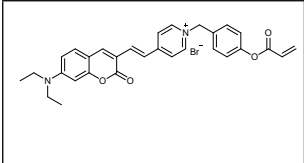
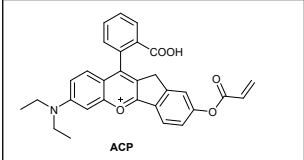


Fig. S9 The confocal images of HepG2 cells: control group; treated with ANTC (30 min); pretreated with NEM (1 h) and then treated with ANTC (30 min); pretreated with NEM (1 h), treated with Cys, Hcy and GSH (1 h) and then ANTC (30 min). Concentration: ANTC 10 µM, NEM 1 mM, Cys 200 µM, Hcy 10 µM and GSH 1mM. Excitation at 633 nm. Collected at 680-759 nm. Scale bar: 20 µm.

Table S1 Property comparisons of some recently reported probes with the acrylate group as the recognition site in the presence of Cys.

Probe	Year	λ_{abs} (nm)	λ_{em} (nm)	Response time (min)	Response mode	LOD (μM)	Application	Ref.
 ANTC	2021	690	727	1.5	Turn-on	0.21	Cell and mouse	This work
 NTC	2021	556	665	20	Turn-on	–	Cell and zebrafish	[6]
 Myco-Cys	2021	417	517	60	Turn-on	0.045	Cell	[7]
 TIA	2020	496	540	5	Turn-on	0.11	Cell	[8]
 SHCy-C	2020	728	770	5	Turn-on	0.021 2	Cell	[9]
 Cys-WR	2019	543	653	40	Turn-on	0.83	Cell and zebrafish	[10]
 Cy-OAc	2019	769, 505	794, 635	30	Ratiometric	0.09	Cell and mouse	[11]
 IPPA	2019	330	375	12	Turn-on	0.33	Cell and zebrafish	[12]

	2019	508, 452	644, 539	30	Ratiometric	0.046 7	Cell	[13]
	2019	560	610	15	Turn-on	0.024 1	Two-photon imaging in cell and mous	[14]

Reference

- [1] K. Wang, T. Leng, Y. Liu, C. Wang, P. Shi, Y. Shen, W.-H. Zhu, A novel near-infrared fluorescent probe with a large Stokes shift for the detection and imaging of biothiols, *Sens. Actuators, B*. 248 (2017) 338-345.
- [2] H. Lv, H. Sun, S. Wang, F. Kong, A novel dicyanoisophorone based red-emitting fluorescent probe with a large Stokes shift for detection of hydrazine in solution and living cells, *Spectrochim. Acta, Part A* 196 (2018) 160-167.
- [3] X. Shi, F. Huo, J. Chao, Y. Zhang, C. Yin, An isophorone-based NIR probe for hydrazine in real water samples and hermetic space, *New J. Chem.* 43 (2019) 10025-10029.
- [4] R. Lemke, Knoevenagel condensation in dimethylformamide, *Synthesis* 5 (1974) 359-361.
- [5] Y. Zhang, Y. Ma, Z. Wang, X. Zhang, X. Chen, S. Hou, H. Wang, A novel colorimetric and far-red emission ratiometric fluorescent probe for the highly selective and ultrafast detection of hypochlorite in water and its application in bioimaging, *Analyst* 145 (2020) 939-945.
- [6] X. Hou, Z. Li, Y. Li, Q. Zhou, C. Liu, D. Fan, J. Wang, R. Xu, Z. Xu, ICT-modulated NIR water-soluble fluorescent probe with large Stokes shift for selective detection of cysteine in living cells and zebrafish, *Spectrochim Acta Part A* 246 (2021) 119030.
- [7] W. Lee, T. Yudhistira, W. Youn, S. Han, M.B. Halle, J.H. Choi, Y. Kim, I.S. Choi, D.G. Churchill, Inexpensive water soluble methyl methacrylate-functionalized hydroxyphthalimide: variations of the mycophenolic acid core for selective live cell imaging of free cysteine, *Analyst* 146 (2021) 2212-2220.
- [8] Q. Zhang, S. Wang, N. Zhang, S. Chen, K.-P. Wang, Z.-Q. Hu, Acryl-modified diazabenz[ghi]perylene for fast discrimination of Cys from GSH and Hcy with high quantum yield, *Sensors Actuators B: Chem.* 320 (2020) 128304.
- [9] S. Cai, C. Liu, X. Jiao, L. Zhao, X. Zeng, A lysosome-targeted near-infrared fluorescent probe for imaging endogenous cysteine (Cys) in living cells, *J. Mater. Chem. B* 8 (2020) 2269-2274.
- [10] X. Zhang, H. Liu, Y. Ma, W. Qu, H. He, X. Zhang, S. Wang, Q. Sun, F. Yu, Development of a novel near-infrared fluorescence light-up probe with a large Stokes shift for sensing of cysteine in aqueous solution, living cells and zebrafish, *Dyes Pigm.* 171 (2019) 107722.
- [11] X. Zhang, N. He, Y. Huang, F. Yu, B. Li, C. Lv, L. Chen, Mitochondria-targeting near-infrared ratiometric fluorescent probe for selective imaging of cysteine in orthotopic lung cancer mice, *Sensors Actuators B: Chem.* 282 (2019) 69-77.
- [12] M. Zhu, L. Wang, X. Wu, R. Na, Y. Wang, Q.X. Li, B.D. Hammock, A novel and simple imidazo[1,2-a]pyridin fluorescent probe for the sensitive and selective imaging of cysteine in living cells and zebrafish, *Anal. Chim. Acta* 1058 (2019) 155-165.
- [13] D. Zhu, X. Yan, A. Ren, W. Xie, Z. Duan, A novel colorimetric and ratiometric fluorescent probe for cysteine based on conjugate addition-cyclization-elimination strategy with a large Stokes shift and

bioimaging in living cells, *Anal. Chim. Acta* 1058 (2019) 136-145.

[14] D. Liu, Y. Lv, M. Chen, D. Cheng, Z. Song, L. Yuan, X. Zhang, A long wavelength emission two-photon fluorescent probe for highly selective detection of cysteine in living cells and an inflamed mouse model, *J. Mater. Chem. B* 7 (2019) 3970-3975.